The Canadian Mineralogist
Vol. 44, pp. 465-480 (2006)

THE CRYSTAL STRUCTURE OF BERRYITE, $Cu_3Ag_2Pb_3Bi_7S_{16}$

DAN TOPA[§]

Department of Material Science, Division of Mineralogy, University of Salzburg, Hellbrunnerstrasse 34/III, A–5020, Salzburg, Austria

EMIL MAKOVICKY

Geological Institute, University of Copenhagen, Østervoldgade 10, DK–1350 Copenhagen K, Denmark

HUBERT PUTZ

Department of Geography, Geology and Mineralogy, University of Salzburg, Hellbrunnerstrasse 34/III, A–5020, Salzburg, Austria

W. GUS MUMME

CSIRO Minerals, Bayview Avenue, Clayton 3168, Australia

ABSTRACT

The crystal structure of berryite, ideally $Cu_3Ag_2Pb_3Bi_7S_{16}$, monoclinic, *a* 12.703(2), *b* 4.0305(7), *c* 28.925(5) Å, β 102.484(2)°, space group $P2_1/m$, $Z = 2$, $D_{calc} = 6.899$ g/cm^3, has been solved by direct methods and refined to an R_1 index of 6.4% for 2352 unique reflections measured with Mo$K\alpha$ X-radiation on a three-circle diffractometer equipped with a CCD area-detector. There are fifteen unique *Me* sites and sixteen S sites in the asymmetric unit. Three Pb sites and two Bi sites are located on the surfaces of PbS-like slabs four layers thick, of two kinds; four Bi sites and two Ag sites are located in the interior of the slabs. Copper atoms in triangular coordination lie in a single S layer, with pseudohexagonal geometry. One Bi site straddles the interspace between the PbS-like slab and the S–Cu layer. Three primitive pseudotetragonal subcells of the PbS-like slab match with two orthohexagonal subcells of the Cu–S layer; this semicommensurate *lock-in* structure is made possible by the extension of the *a* parameter of the PbS-like slab by insertion of wide AgS_{2+4} octahedra (linear S–Ag–S coordinations). The structure determined allowed us to derive model structures of orthorhombic berryite (a polytypic variant) and of watkinsonite, $Cu_2PbBi_4(Se,S)_8$. Structures of $Ca_2Sb_2S_5$ and $La_4In_5S_{13}$ follow the same modular principles.

Keywords: berryite, sulfosalt, crystal structure, electron-microprobe analysis, Grube Clara, Germany.

SOMMAIRE

Nous avons résolu la structure cristalline de la berryite, de composition idéale $Cu_3Ag_2Pb_3Bi_7S_{16}$, monoclinique, *a* 12.703(2), *b* 4.0305(7), *c* 28.925(5) Å, β 102.484(2)°, groupe spatial $P2_1/m$, $Z = 2$, $D_{calc} = 6.899$ g/cm^3, par méthodes directes, et nous l'avons affinée jusqu'à un résidu R_1 de 6.4% avec 2352 réflexions uniques mesurées au moyen d'un rayonnement Mo$K\alpha$ et d'un diffractomètre à trois cercles muni d'un détecteur à aire de type CCD. Il y a quinze sites uniques *Me* et seize sites S dans la maille élémentaire. Trois sites Pb et deux sites Bi sont situés sur la surface de plaques de type PbS à quatre couches, et de deux types; quatre sites Bi et deux sites Ag sont situés à l'intérieur de ces plaques. Les atomes de Cu en coordinence triangulaire sont situés dans une couche d'atomes S ayant une symétrie pseudohexagonale. Un site Bi chevauche l'espace interfoliaire entre les plaques de type PbS et le niveau S–Cu. Trois sous-mailles pseudotétragonales primitives de la plaque de type PbS sont raccordées à deux sous-mailles orthohexagonales de la couche Cu–S; cette structure semi-commensurable intégrée est rendue possible par l'extension du paramètre *a* de la plaque de type PbS par l'insertion de larges octaèdres AgS_{2+4} (coordinence S–Ag–S linéaire). La structure déterminée nous permet de dériver des modèles structuraux de la berryite orthorhombique (variante polytypique) et de la watkinsonite, $Cu_2PbBi_4(Se,S)_8$. Les structures de $Ca_2Sb_2S_5$ et de $La_4In_5S_{13}$ répondent aux mêmes principes modulaires.

(Traduit par la Rédaction)

Mots-clés: berryite, sulfosel, structure cristalline, analyses à la microsonde électronique, Grube Clara, Allemagne.

§ *E-mail address*: dan.topa@sbg.ac.at

Introduction

Berryite was first described and named by Nuffield & Harris (1966) from two type localities, the Nordmark mines, Sweden, and the Missouri mine, Colorado. The formula given in this original description was $Pb_2(Cu,Ag)_3Bi_5S_{11}$; this formula also was favored in the description of berryite from Owen Lake, British Columbia (Harris & Owens 1973).

In his description of berryite from Ivigtut, Greenland, Karup-Møller (1966) proposed the formula $Pb_3(Cu_{3.5}Ag_{1.5})Bi_7S_{16}$, on the basis of results of electron-microprobe analyses. He also recognized the pseudo-orthorhombic geometry of the monoclinic lattice of berryite. Further descriptions of berryite were given by Borodayev & Mozgova (1971) from three deposits in central Asia, Karup-Møller (1977) from Greenland, and Foord *et al.* (1988) from the Fairview mine, Nevada. More recent electron-microprobe analyses of berryite were reported by Cook (1998) and Gu *et al.* (2001). Crystallographic data were given by Nuffield & Harris (1966) and Karup-Møller (1966); W.G. Mumme and E. Makovicky obtained information in the 1990s, but it was not published. The crystal structure of berryite has remained unknown.

In the mid-1990s, berryite was identified by qualitative energy-dispersion spectrometry and X-ray powder-diffraction methods in material from the Grube Clara, Black Forest, Germany (Walenta 1995). It occurs as needle-like crystals up to 5 mm in length in quartz cavities, associated with fluorite and chalcopyrite. A new find of well-developed, free isolated crystals of berryite in the material from Grube Clara allowed us to perform a structure determination on this mineral.

Experimental

Chemical analysis

A needle-like fragment was extracted from the aggregate shown in Figure 1a. The fragment was split, and one half, after polishing, was used for optical microscopy and electron-microprobe investigations (Figs. 1b, d), whereas the other half was used for single-crystal investigation of the structure.

Quantitative chemical analyses were performed with a JEOL JXA–8600 electron microprobe (controlled by Advance Microbeam system of programs), operated at 25 kV and 40 nA, with a counting time of 20 s for peaks and 7 s for background. The following natural (n) and synthetic (s) standards and X-ray lines were used: n–$CuFeS_2$ (Cu$K\alpha$, Fe$K\alpha$), s–Bi_2S_3 (Bi$L\alpha$, S$K\alpha$), n–PbS (Pb$L\alpha$), s–CdTe (Cd$L\alpha$, Te$L\alpha$), n–Sb_2S_3 (Sb$L\alpha$) and pure metal for Ag$L\alpha$. Raw data were corrected with the on-line ZAF procedure. Standard deviations (error in wt. %) of elements sought in berryite are: Bi 0.18, Pb 0.19, S 0.06, Te and Se 0.04, Cu, Ag and Se 0.03.

Results of ten point-analyses randomly distributed over the aggregate in Figure 1d were averaged. Chemical data pertaining to the material used for the structural study as well as to berryite from other occurrences and the literature data are compiled in Table 1, and plotted in the diagram Bi–(Ag,Cu)–Pb (Fig. 2).

Single-crystal X-ray diffraction

A fragment of berryite with an irregular shape from Grube Clara was measured on a Bruker AXS three-circle diffractometer equipped with a CCD area detector using graphite-monochromated Mo$K\alpha$ radiation. Crystal data are listed in Table 2. The Smart (Bruker AXS, 1998) system of programs was used for unit-cell determination and data collection, Saint+ (Bruker AXS, 1998) for the calculation of integrated intensities, and Xprep (Bruker AXS, 1998) for empirical absorption-correction based on pseudo Ψ-scans. The centrosymmetric space-group $P2_1/m$ proposed by the Xprep program was chosen, and it is consistent with the monoclinic symmetry of the lattice and intensity statistics (mean $|E^2 - 1| = 0.988$). The structure was solved by direct methods (program Shelxs97, Sheldrick 1997a), which revealed most of the cation positions. In the subsequent cycles of the refinement (program SHELXL97 Sheldrick 1997b), cation positions were deduced from difference-Fourier syntheses by selecting among the strongest maxima at appropriate distances.

Experimental details of the data collection and refinement are given in Table 2, fractional coordinates, isotropic and anisotropic displacement parameters of the atoms are listed in Table 3, and selected *Me*–S bond distances are presented in Table 4. Selected geometrical parameters for individual coordination-polyhedra (Balić-Žunić & Makovicky 1996, Makovicky & Balić-Žunić 1998), calculated with the Ivton program (Balić-Žunić & Vicković 1996), are given in Table 5. The structure of berryite is presented in Figure 3, the site labeling in Figure 4, and the coordination polyhedra in Figure 5. The table of structure factors may be obtained from the Depository of Unpublished Data, CISTI, National Research Council, Ottawa, Ontario K1A 0S2, Canada.

Chemical Composition

Table 1 shows that the results of the first electron-microprobe analyses of berryite (Karup-Møller 1966, Harris & Owens 1973) differ substantially from more recent results, even where the same material was analyzed (*e.g.*, Karup-Møller 1977). Based on the personal experience of one of the authors (E.M.), these deviations are clearly a product of the imperfect state of correction procedures of electron-microprobe-produced analytical data on sulfides in the sixties and early seventies. Therefore, results of the early analyses are to be disregarded.

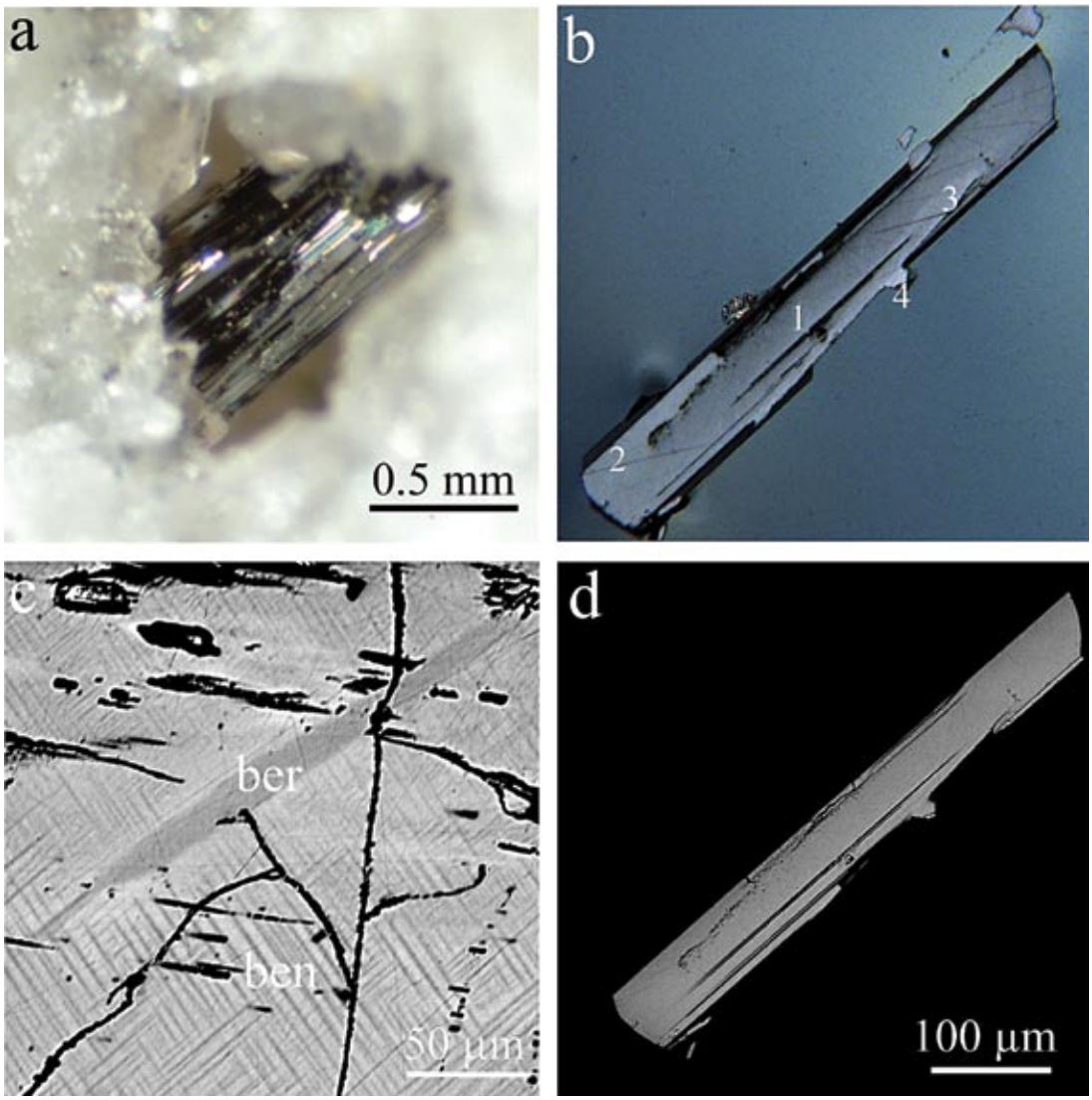

FIG. 1. Optical and back-scattered-electron images of berryite: a) aggregate of berryite in a cavity in quartz from Grube Clara, b) optical image of the aggregate of berryite analyzed (crossed polars), with four differently oriented components, c) a berryite lamella in a matrix of exsolved benjaminite from the Silverton District, Colorado, USA, d) back-scattered-electron image of berryite aggregate from Figure 1b.

The analytical results for berryite from Grube Clara, the Mike mine and Silverton District, Colorado (Table 1, Fig. 2) are tightly clustered and positioned close to the structurally determined stoichiometry, $Cu_3Ag_2Pb_3Bi_7S_{16}$. The somewhat higher Bi values for the sample from the Silverton District, Colorado, may be due to contamination by surrounding Cu-rich benjaminite (dark lamellae: Cu 5.1, Ag 8.0, Pb 11.6, Bi 57.6, Se 0.4, S17.3, total 100.0 wt.%, and bright lamellae: Cu 2.1, Ag 10.8, Pb 6.8, Bi 62.4, Se 0.2, S17.5, total 99.8 wt.%) (Fig. 1c). The results of Cook (1998) and Gu *et al.* (2001) show considerable spread at right angles to one another in Figure 2.

TABLE 1. AVERAGE RESULTS OF ELECTRON-MICROPROBE ANALYSES OF BERRYITE FROM VARIOUS LOCALITIES

No.	Sample	N.A.	Cu	Ag	Fe	Pb	Bi	Te	Se	S	Total	Ref.
1	Berryite: ideal formula		6.35	7.18	-	20.69	48.70	-	-	17.08	100.00	
2	Ivigtut, Greenland, No.1		7.10	4.90	-	21.60	49.20	-	-	17.20	100.00	1
3	Ivigtut, Greenland, No.2		7.40	6.10	-	21.00	48.40	-	-	17.10	100.00	1
4	Ivigtut, Greenland, No.3		7.80	6.80	-	20.80	47.50	-	-	17.20	100.10	1
5	Owen Lake, British Columbia	5	5.3(1)	7.4(3)	-	20.9(5)	49.5(5)	-	-	17.0(5)	100.10	2
6	Ivigtut, Greenland, No. A	9	6.1(1)	6.8(1)	-	21.6(8)	48.9(1.4)	-	-	17.2(3)	100.60	3
7	Manhattan, Nevada, No. B	9	5.8(1)	6.7(2)	-	19.5(5)	48.3(6)	-	-	17.3(1)	97.60	3
8	Băiuţ-Văratec, Romania, (1)		6.81	5.67	0.26	21.29	46.47	0.19	2.13	16.02	98.80	4
9	Băiuţ-Văratec, Romania, (2)		6.03	7.14	0.11	20.79	46.74	0.11	2.22	15.93	99.19	4
10	Băiuţ-Văratec, Romania, (3)		5.80	8.54	0.00	19.30	48.39	0.12	1.95	16.11	100.27	4
11	Băiuţ-Văratec, Romania, (4)		6.83	6.96	0.26	20.50	47.37	0.00	1.88	16.42	100.22	4
12	Băiuţ-Văratec, Romania, (5)		7.45	7.45	0.25	19.68	46.68	0.00	1.78	16.39	99.68	4
13	Funiushan, China, e12		7.27	6.43	0.36	19.96	47.67	0.05	2.86	15.37	99.95	5
14	Funiushan, China, e29		7.59	6.95	0.35	19.10	46.19	0.45	2.86	15.63	99.12	5
15	Funiushan, China, e30		7.74	7.75	0.41	19.50	45.41	0.94	2.77	15.57	100.09	5
16	Silverton District, Colorado	5	5.96(8)	7.01(12)	-	19.94(14)	49.59(12)	0.00	0.26(4)	16.94(4)	99.70(23)	6
17	Mike mine, San Juan, Colorado	4	6.14(2)	7.04(15)	-	20.47(10)	48.81(2)	0.11(2)	0.32(3)	16.95(4)	99.84(8)	6
18	Grube Clara, Germany	10	6.18(6)	6.88(14)	-	20.90(13)	49.04(15)	0.00	0.00	17.08(9)	100.09(26)	7

Chemical formulae based on 31 atoms

1) $Cu_{3.00}Ag_{2.00}Pb_{3.00}Bi_{7.00}S_{16.00}$
2) $Cu_{3.35}Ag_{1.36}Pb_{3.13}Bi_{7.06}S_{16.09}$
3) $Cu_{3.47}Ag_{1.69}Pb_{3.02}Bi_{6.91}S_{15.91}$
4) $Cu_{3.62}Ag_{1.86}Pb_{2.96}Bi_{6.71}S_{15.84}$
5) $Cu_{2.53}Ag_{2.09}Pb_{3.07}Bi_{7.20}S_{16.11}$
6) $Cu_{2.88}Ag_{1.89}Pb_{3.13}Bi_{7.02}S_{16.09}$
7) $Cu_{2.78}Ag_{1.89}Pb_{2.87}Bi_{7.04}S_{16.43}$
8) $Cu_{3.27}Ag_{1.59}Pb_{3.27}Bi_{6.78}(S_{15.23}Se_{0.82}Te_{0.05})_{\Sigma16.09}$
9) $Cu_{2.90}Ag_{2.02}Pb_{3.13}Bi_{6.87}(S_{15.19}Se_{0.86}Te_{0.03})_{\Sigma16.08}$
10) $Cu_{2.76}Ag_{2.40}Pb_{2.82}Bi_{7.03}(S_{15.21}Se_{0.75}Te_{0.03})_{\Sigma15.99}$
11) $Cu_{3.21}Ag_{1.93}Pb_{3.09}Bi_{6.77}(S_{15.29}Se_{0.71})_{\Sigma16.00}$
12) $Cu_{3.48}Ag_{2.05}Pb_{2.96}Bi_{6.64}(S_{15.20}Se_{0.67})_{\Sigma15.87}$
13) $Cu_{3.47}Ag_{1.81}Pb_{3.12}Bi_{6.93}(S_{14.56}Se_{1.10}Te_{0.01})_{\Sigma15.67}$
14) $Cu_{3.59}Ag_{1.94}Pb_{2.96}Bi_{6.65}(S_{14.66}Se_{1.09}Te_{0.11})_{\Sigma15.86}$
15) $Cu_{3.63}Ag_{2.14}Pb_{3.02}Bi_{6.47}(S_{14.47}Se_{1.05}Te_{0.22})_{\Sigma15.73}$
16) $Cu_{2.84}Ag_{1.97}Pb_{2.91}Bi_{7.18}(S_{15.99}Se_{0.10})_{\Sigma16.09}$
17) $Cu_{2.92}Ag_{1.97}Pb_{2.98}Bi_{7.04}(S_{15.94}Se_{0.10}Te_{0.03})_{\Sigma16.07}$
18) $Cu_{2.93}Ag_{1.92}Pb_{3.04}Bi_{7.07}S_{16.04}$

The raw data are quoted in wt.%. N.A.: number of analyses.
References: 1) Karup-Møller (1966), 2) Harris & Owens (1973), 3) Karup-Møller (1977), 4) Cook (1998), 5) Gu *et al.* (2001), 6) D. Topa (unpubl. data), 7) this study.

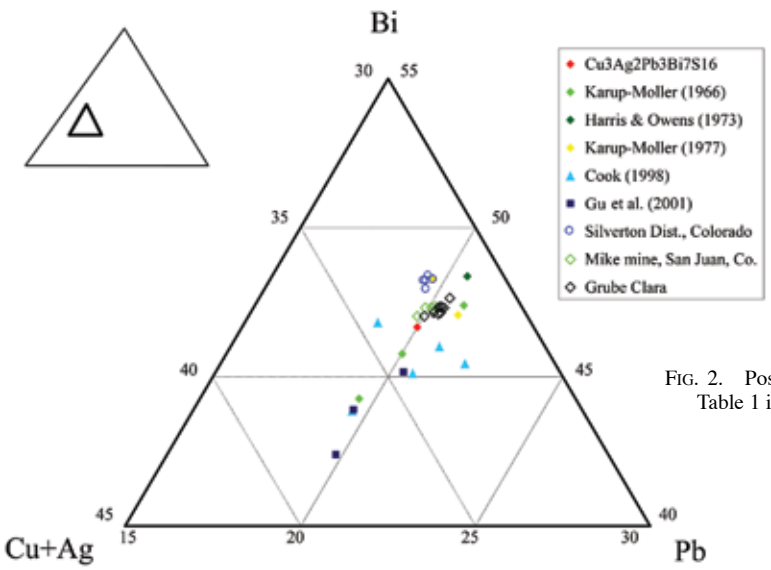

FIG. 2. Position of berryite compositions from Table 1 in the diagram (Cu,Ag)–Pb–Bi.

DESCRIPTION OF THE STRUCTURE

Coordination polyhedra

The crystal structure of berryite contains three distinct Pb positions, seven Bi sites, two Ag sites and three distinct Cu sites (Table 3). Sixteen distinct sulfur sites complete the picture. Atoms Pb1 and Pb2 are situated on the surfaces of the PbS-like slabs (pseudotetragonal Q_1 and Q_2 slabs in Fig. 6), whereas four bismuth sites (Bi2, Bi6, Bi3 and Bi7) and silver sites (Ag1 and Ag2) lie in the slab interior. Two more Bi sites (Bi5 and Bi4) are on the slab surfaces, adjacent to the Pb polyhedra. The remaining Bi1 site straddles the interspace between the slab and a pseudohexagonal layer (H in Fig. 6) built of single sulfur atoms (S1, S3, S9, S12) and triangular copper sites (Cu1, Cu2 and Cu3).

All three Pb sites form slightly asymmetric bicapped trigonal-coordination prisms (Table 4, 5). The least asymmetric site is Pb3; it is a position drawn from the PbS-like slab and paired with interlayer Bi1 into columns straddling the interspace. Asymmetry of Pb1 and Pb2 is caused by the fact that they are embedded in the PbS-like layer.

Considering the distribution of the short bonds (Table 4), the surface sites Bi4 and Bi5 have square coordination-pyramids oriented toward the interlayer of single sulfur atoms, *i.e.*, into the interlayer space. Their indistinctly expressed lone-electron pairs point toward the PbS-like slab. The central Bi sites participate in elongate oval lone-electron-pair micelles along the median planes of the PbS-like slabs: the Bi2 and Bi3 sites are situated close to the largest opening of these micelle spaces, and as a consequence, are most asymmetric (Table 4, 5). The Bi6 sites are closer to the ends of the micelle and are forced into a more symmetrical coordination. In the case of Bi7, a more symmetrical coordination appears to be forced by the accommodation of the adjacent, most asymmetric Bi1 (Table 4, 5).

TABLE 2. X-RAY DIFFRACTION (SINGLE CRYSTAL): EXPERIMENTAL DETAILS

Crystal data	
Chemical formula	$Cu_3Ag_2Pb_3Bi_7S_{16}$
Chemical formula weight	3003.75
Cell setting	Monoclinic
Space group	$P2_1/m$
a (Å)	12.703(2)
b (Å)	4.0305(7)
c (Å)	28.925(5)
β (°)	102.484(2)
V (Å^3)	1445.9(4)
Z	2
D_x (g/cm^3)	6.899
Radiation type	Mo $K\alpha$
Wavelength (Å)	0.71073
No. of reflections for cell parameters	2545
μ (mm^{-1})	64.44
Temperature (K)	297(1)
Crystal habit	needle
Crystal size (mm)	0.015 × 0.025 × 0.100
Crystal color	metallic
Data collection	
Absorption correction	empirical (ellipsoidal function)
T_{min}	0.1773
T_{max}	0.3848
No. of measured reflections	8648
No. of independent reflections	2352
No. of observed reflections	2072
Criterion for observed reflections	$I > 2\sigma(I)$
R_{int}	8.44%
θ_{max} (°)	23.34
Range of h, k, l	$-14 < h < 13$, $-4 < k < 4$, $-32 < l < 32$
Refinement	
Refinement	on F_o^2
R [$F_o^2 > 2\sigma(F_o^2)$]	6.40%
wR (F_o^2)	14.17%
S (GooF)	1.174
No. of reflections used in refinement	2167
No. of parameters refined	187
Weighting scheme	$w = 1/[\sigma^2(F_o^2) + (0.0654P)^2 + 57.3P]$ where $P = (F_o^2 + 2F_c^2)/3$
$(\Delta/\sigma)_{max}$	0.000
$\Delta\rho_{max}$ (e/Å^3)	3.93 (1.01 Å from Pb3)
$\Delta\rho_{min}$ (e/Å^3)	-3.92 (1.53 Å from Bi1)
Extinction method	none
Source of atomic scattering factors	International Tables for X-Ray Crystallography (1992, Vol. C, Tables 4.2.6.8 and 6.1.1.4)
Computer programs	
Structure solution	SHELXS97 (Sheldrick 1997a)
Structure refinement	SHELXL97 (Sheldrick 1997b)

TABLE 3. ATOM PARAMETERS FOR BERRYITE

Atom	x/a	z/c	U_{11}	U_{22}	U_{33}	U_{13}	U_{eq}
Bi1	0.01029(12)	0.19285(5)	0.0149(9)	0.0070(8)	0.0160(8)	0.0015(6)	0.0129(4)
Bi2	0.05234(12)	0.44385(5)	0.0138(9)	0.0070(8)	0.0134(8)	0.0033(6)	0.0113(4)
Bi3	0.23842(12)	0.95422(5)	0.0143(8)	0.0051(7)	0.0147(8)	0.0053(6)	0.0111(4)
Bi4	0.52225(12)	0.64744(5)	0.0117(8)	0.0036(7)	0.0153(8)	0.0043(6)	0.0100(4)
Bi5	0.63580(12)	0.14436(5)	0.0138(8)	0.0051(7)	0.0124(8)	0.0018(6)	0.0106(4)
Bi6	0.71532(12)	0.45283(5)	0.0148(9)	0.0045(7)	0.0167(8)	0.0038(7)	0.0119(4)
Bi7	0.89915(12)	0.94336(5)	0.0147(9)	0.0067(8)	0.0162(8)	0.0054(6)	0.0123(4)
Pb1	0.18898(13)	0.66000(6)	0.0220(9)	0.0098(8)	0.0210(9)	0.0045(7)	0.0177(4)
Pb2	0.32335(14)	0.16151(6)	0.0251(9)	0.0105(8)	0.0233(9)	0.0048(7)	0.0197(4)
Pb3	0.86159(13)	0.67228(6)	0.0176(8)	0.0110(8)	0.0203(9)	0.0068(7)	0.0159(4)
Ag1	0.3872(3)	0.4502(1)	0.039(3)	0.076(3)	0.014(2)	0.005(2)	0.043(1)
Ag2	0.5636(3)	0.9483(1)	0.037(2)	0.078(3)	0.016(2)	0.001(2)	0.044(1)
Cu1	0.2212(4)	0.7650(2)	0.021(3)	0.012(3)	0.031(3)	0.007(2)	0.021(1)
Cu2	0.5349(4)	0.2603(2)	0.025(3)	0.013(3)	0.040(4)	0.016(3)	0.024(1)
Cu3	0.7355(4)	0.7580(2)	0.014(3)	0.008(3)	0.038(3)	0.009(2)	0.019(1)
S1	0.0397(7)	0.7526(3)	0.007(5)	0.007(5)	0.010(5)	0.005(4)	0.008(2)
S2	0.1232(8)	0.5587(4)	0.004(5)	0.012(5)	0.024(6)	0.003(4)	0.013(2)
S3	0.1872(8)	0.2548(4)	0.008(5)	0.006(5)	0.022(6)	0.004(4)	0.012(2)
S4	0.2082(9)	0.8606(3)	0.022(6)	0.011(5)	0.003(5)	0.007(7)	0.012(2)
S5	0.2545(8)	0.0613(3)	0.008(5)	0.014(5)	0.006(5)	0.001(4)	0.010(2)
S6	0.3434(8)	0.3637(3)	0.007(5)	0.003(5)	0.013(5)	-0.001(4)	0.008(2)
S7	0.4228(9)	0.5368(4)	0.025(6)	0.008(5)	0.019(6)	0.008(5)	0.017(2)
S8	0.5215(8)	0.8613(4)	0.012(6)	0.010(5)	0.023(6)	0.005(5)	0.015(2)
S9	0.5542(8)	0.7393(4)	0.010(5)	0.014(5)	0.016(5)	0.006(4)	0.013(2)
S10	0.6118(9)	0.0359(4)	0.017(6)	0.019(6)	0.014(5)	-0.001(5)	0.017(2)
S11	0.6562(7)	0.3562(4)	0.004(5)	0.004(5)	0.020(5)	0.001(4)	0.010(2)
S12	0.6965(8)	0.2368(4)	0.016(6)	0.005(5)	0.017(5)	0.002(4)	0.013(2)
S13	0.8022(8)	0.5574(3)	0.006(5)	0.012(5)	0.010(5)	-0.005(4)	0.010(2)
S14	0.8568(9)	0.8470(4)	0.022(6)	0.011(5)	0.011(5)	0.008(4)	0.014(2)
S15	0.9326(9)	0.0492(4)	0.019(6)	0.008(5)	0.021(6)	0.013(6)	0.015(2)
S16	0.9918(9)	0.3526(4)	0.022(6)	0.001(4)	0.017(5)	0.011(4)	0.012(2)

For all atoms, $y/b = ½$ and $U_{23} = U_{12} = 0$ by symmetry.

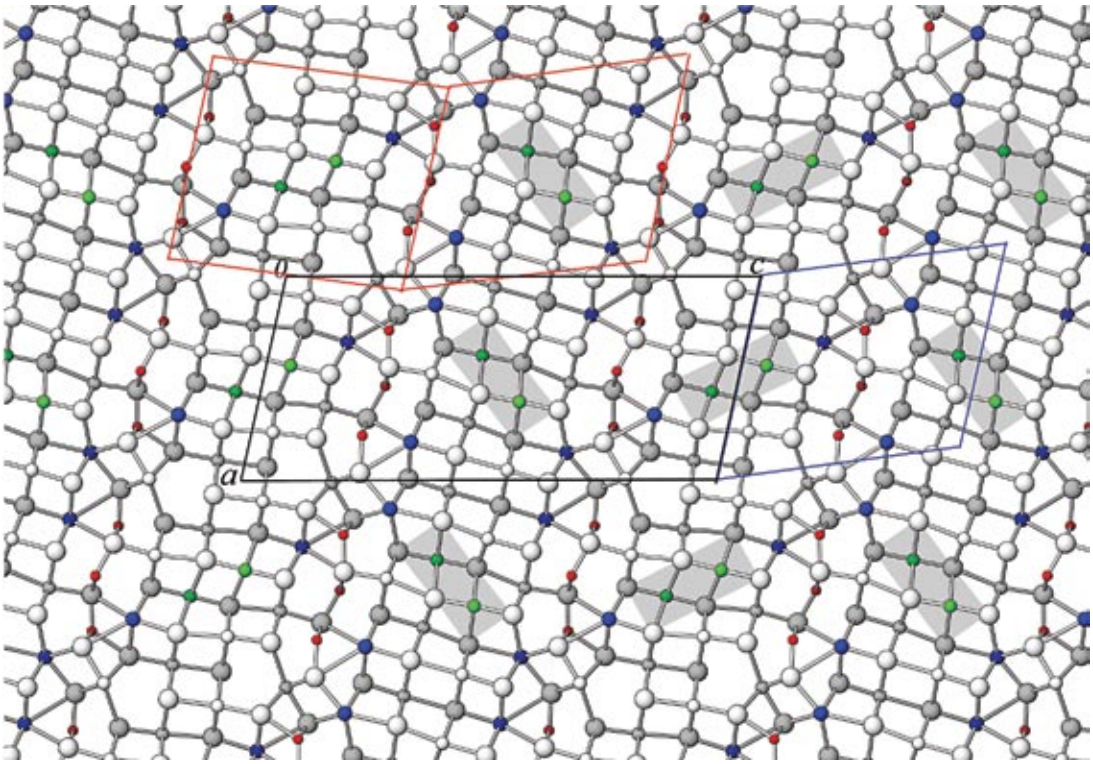

FIG. 3. Crystal structure of berryite in projection along the *b* axis, with atoms at $y = ¼$ (lighter colors) and ¾ (darker colors), respectively. In order of decreasing size, circles represent S, Pb (blue), Ag (green), Bi, and Cu (red). Black outline: unit cell of berryite; red: "component subcells" of the two alternating (001) layer types; the "unit cell" of watkinsonite coincides with red right-hand subcell (details in the text); blue: the "unit cell" of the polytype layer.

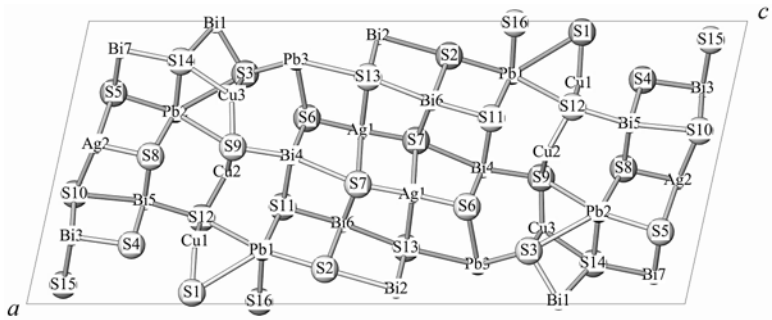

FIG. 4. Unit-cell contents of berryite. The *a* axis points downward, the *c* axis points to the right. Symbols as in Figure 3.

The Ag1 and Ag2 sites, in a flat-octahedral 2 + 4 coordination, divide the Pb-like slabs into regular intervals. The two short bonds of the linear two-fold coordination are 2.44–2.47 Å long, whereas the remaining four "perpendicular" distances are equal to 3.10–3.12 Å. The linear bonds comprise the angle of 178.1 and 177.7°, respectively, for the above Ag sites. Among the three trigonal planar sites, Cu1 has the shortest Cu–S bonds (2.25–2.28 Å), whereas the Cu2 and Cu3 positions display slightly longer distances (2.25–2.31 Å); the Cu3 site shows a trend toward tetrahedral coordination, with an additional Cu–S distance of 2.70 Å. All

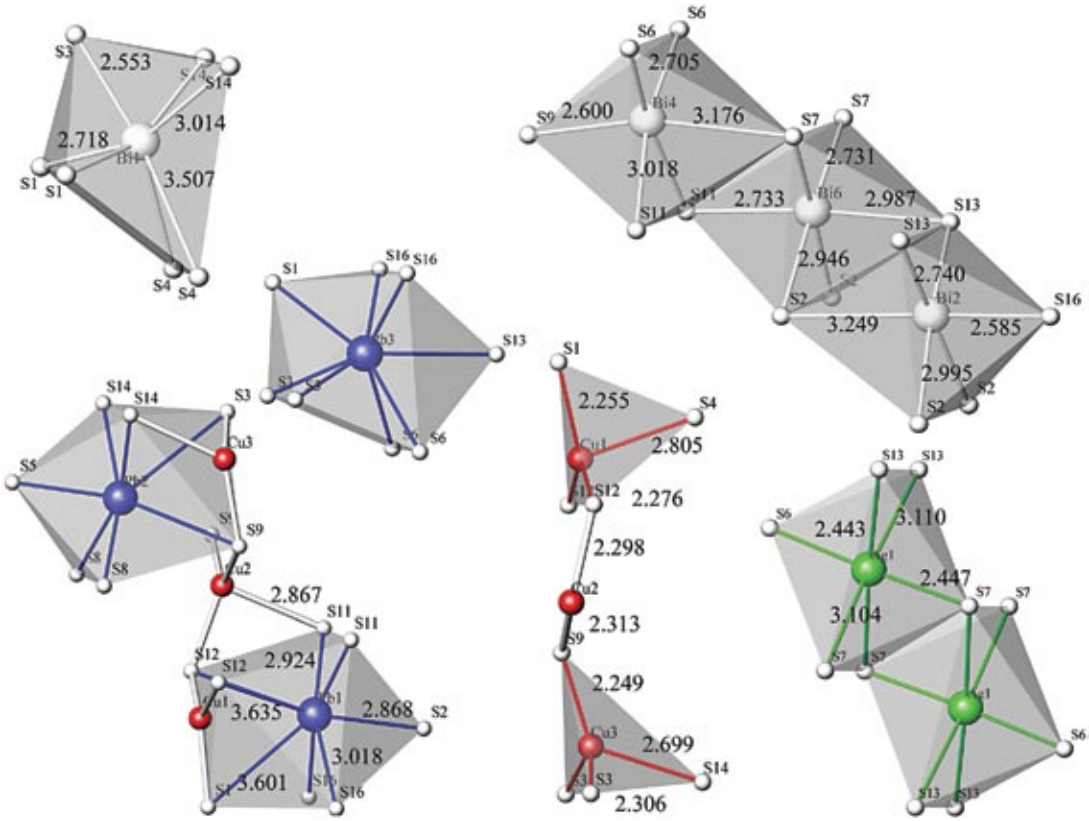

FIG. 5. Coordination polyhedra for Cu, Ag, Pb and Bi in berryite.

TABLE 4. SELECTED INTERATOMIC DISTANCES (Å) IN BERRYITE

Bi1		Bi2		Bi3		Bi4		Bi5		Bi6		Bi7	
S3	2.553(10)	S16	2.585(11)	S4	2.652(9)	S9	2.600(9)	S12	2.618(8)	S7	2.731(8)	S14	2.722(9)
S1	2.718(6)	S13	2.740(7)	S10	2.744(8)	S6	2.705(6)	S8	2.818(7)	S7	2.731(8)	S5	2.788(7)
S1	2.718(6)	S13	2.740(7)	S10	2.744(8)	S6	2.705(6)	S8	2.818(7)	S11	2.733(9)	S5	2.788(7)
S14	3.014(9)	S2	2.995(8)	S15	2.949(9)	S11	3.018(7)	S4	2.852(7)	S2	2.946(8)	S15	2.911(8)
S14	3.014(9)	S2	2.995(8)	S15	2.949(9)	S11	3.018(7)	S4	2.852(7)	S2	2.946(8)	S15	2.911(8)
S4	3.507(8)	S2	3.249(11)	S5	3.060(9)	S7	3.176(11)	S10	3.086(12)	S13	2.987(8)	S15	2.998(12)
S4	3.507(8)												
Pb1		Pb2		Pb3		Ag1		Ag2		Cu1		Cu3	
S2	2.868(11)	S5	2.841(9)	S1	2.871(8)	S6	2.443(9)	S8	2.457(12)	S1	2.255(10)	S9	2.249(11)
S11	2.924(7)	S8	2.991(8)	S16	2.937(8)	S7	2.447(12)	S10	2.475(12)	S12	2.276(5)	S3	2.306(6)
S11	2.924(7)	S8	2.991(8)	S16	2.937(8)	S7	3.104(9)	S10	3.111(10)	S12	2.276(5)	S3	2.306(6)
S16	3.018(8)	S14	3.019(9)	S3	3.076(9)	S7	3.104(9)	S10	3.111(10)	S4	2.805(11)	S14	2.699(10)
S16	3.018(8)	S14	3.019(9)	S3	3.076(9)	S13	3.110(8)	S5	3.123(9)	Cu2			
S1	3.601(10)	S3	3.506(12)	S13	3.245(9)	S13	3.110(8)	S5	3.123(9)	S12	2.298(12)		
S12	3.635(7)	S9	3.575(7)	S6	3.279(7)					S9	2.313(6)		
S12	3.635(7)	S9	3.575(7)	S6	3.279(7)					S9	2.313(6)		
										S11	2.867(10)		

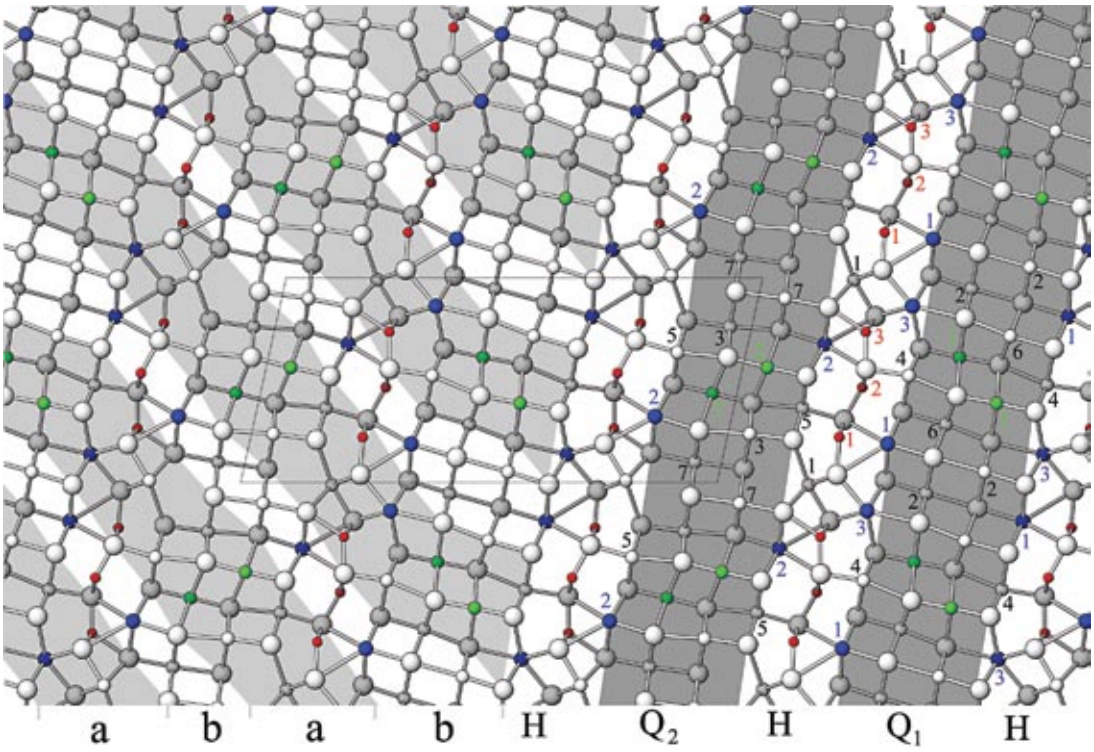

FIG. 6. Right-hand part: Pseudotetragonal four-layer slabs (Q) and pseudohexagonal (H) interlayers in berryite. Left-hand part: the pavonite-type component in berryite (shaded), interleaved with additional structural layers (white).

TABLE 5. POLYHEDRON CHARACTERISTICS FOR BERRYITE

Atom	Volume eccentricity	Sphere radius	Sphere volume	Volume sphericity	Polyhedron volume	Volume distortion
Bi1	0.5119	3.068	121.005	0.9454	36.757	0.1973
Bi2	0.3530	2.902	102.347	0.9840	31.804	0.0237
Bi3	0.2389	2.847	96.699	0.9948	30.735	0.0015
Bi4	0.3354	2.856	97.576	0.9889	31.004	0.0018
Bi5	0.2295	2.838	95.735	0.9902	30.308	0.0054
Bi6	0.2004	2.845	96.446	0.9903	30.594	0.0034
Bi7	0.1591	2.855	97.498	0.9931	30.929	0.0034
Pb1	0.4169	3.177	134.371	0.8946	56.227	0.0347
Pb2	0.3812	3.170	133.476	0.9297	55.851	0.0347
Pb3	0.2312	3.090	123.601	0.9815	51.970	0.0300
Ag1	0.0169	2.886	100.690	0.6448	30.865	0.0370
Ag2	0.0266	2.899	102.098	0.6523	31.173	0.0408
Cu1	0.4886	2.347	54.186	0.9999	6.435	0.0306
Cu2	0.4843	2.399	57.827	1.0000	6.982	0.0146
Cu3	0.3741	2.374	56.063	0.9999	6.282	0.0855

three positions are slightly non-planar. The sum of three central S–Cu–S angles is 350.1, 357.3 and 358.8° for Cu3, Cu2 and Cu1, respectively, as compared to 360° for the perfectly planar coordination.

The Cu and Ag assume very different roles in the crystal structure of berryite. A similar feature was already observed for the structure of neyite (Makovicky *et al.* 2001). The structural formula of berryite, $Pb_3Bi_7Ag_2Cu_3S_{16}$ ($Z = 2$), is in very good agreement with the formula derived by Karup-Møller (1966).

Modular description

The structure of berryite shows modular affinities with (1) the non-commensurate structure of the Pb–Bi sulfosalt cannizzarite, and (2) the pavonite homologous series.

In the first category (1) of modular description of the berryite structure (Fig. 6, right-hand side), pseudotetragonal slabs that are four atom layers thick alternate with single-atom thick pseudohexagonal layers, in analogy to the (thinner) pseudotetragonal and (substantially thicker) pseudohexagonal layers in cannizzarite (Matzat 1979). In berryite, the pseudotetragonal slabs are populated by Pb, Bi and Ag in separate octahedral to semi-octahedral sites, whereas the pseudohexagonal layers contain the triangular copper sites. According to

the composition of surface layers (2Pb + Bi *versus* 2Bi + Pb), two slightly different pseudotetragonal slabs Q_1 and Q_2 alternate in the *c* direction of berryite.

In the interface of pseudotetragonal slabs and pseudohexagonal layers, three primitive pseudotetragonal subcells match with two centered, orthohexagonal subcells along the *a* direction (Fig. 7). Away of the three pseudotetragonal subcells, two are approximately square in shape, whereas the third one, representing the protruding Bi or Pb site, is rectangular. Two triangular copper coordinations are regular, whereas the third one is extended along the [100] direction. The triangular portions corresponding to the protruding (Bi, Pb) atoms are foreshortened in the [100] direction (Fig. 7).

In cannizzarite, a pure Pb–Bi sulfosalt (Matzat 1979), an approximate match between layers is achieved with five primitive pseudotetragonal subcells and three centered pseudohexagonal subcells. The change in the match ratio between cannizzarite and berryite is caused especially by a regular insertion of broad Ag octahedra in the pseudotetragonal slab, connected with the extension of this slab in the *a* direction and the elongation of the coordination rectangles of the protruding (Bi, Pb) atoms situated above the Ag octahedra (Fig. 7).

What is typical of berryite is the position of Bi and, to a lesser extent, Pb, in the interlayer space (Fig. 6), both of which protrude out of the pseudotetragonal slab. Such positions are absent in cannizzarite (Matzat 1979) and contribute to the exact, *lock-in* character of the semicommensurate (Makovicky & Hyde 1992) interlayer match in berryite, in contrast to the very complicated and potentially non-commensurate match in cannizzarite.

In relation (2) to the pavonite homologous series (Makovicky *et al*. 1977, Makovicky 1997), the berryite structure can be modeled as an intergrowth of (a) oblique slices of pavonite-like structure, one half of the pavonite *a* parameter in thickness, with (b) layers one to one and a half octahedron thick composed of octahedrally coordinated large cations with interspersed trigonally coordinated copper sites (Fig. 6, left-hand side).

The exact delineation of pavonite-like slices is arbitrary; the simplest choice is shown in Figure 6. The pairing of square coordination pyramids of Bi with bicapped coordination prisms of Pb leads in these slices to a structural analogy with cupromakovickyite and cupropavonite rather than to that with pavonite, in which only paired Bi pyramids occur in the thin, non-accretional layers (Topa *et al*. 2006). Alternation of (Bi, Pb) pairs with (Pb, Bi) pairs leads to a two-slab periodicity in cupromakovickyite, just as it does in berryite.

If one eliminates the interlayers between cupropavonite-like slices by means of crystallographic shear, a compact cupropavonite-like structure is obtained (Fig. 8). In the shearing process, the heights of atoms in adjacent slices have to be adjusted by 2 Å shifts along the 4 Å direction of the berryite structure. The columns of octahedra in the non-accretional thin layers in the model pavonite homologue derived from berryite are recreated by slicing and joining the Cu-containing polyhedra of the pseudohexagonal layer in berryite.

Derivation of a cupropavonite-like structure from the above-mentioned alternating, slightly different pseudotetragonal slabs in berryite ("Bi–Bi" and "Pb–Pb" slabs if their contributions to the interlayer coordinations are referred to) results in a structure that is a regular intergrowth of two different pavonite homologues: $N_p = 6$ for the Bi–Bi decorated slabs, whereas $N_p = 5$ for the

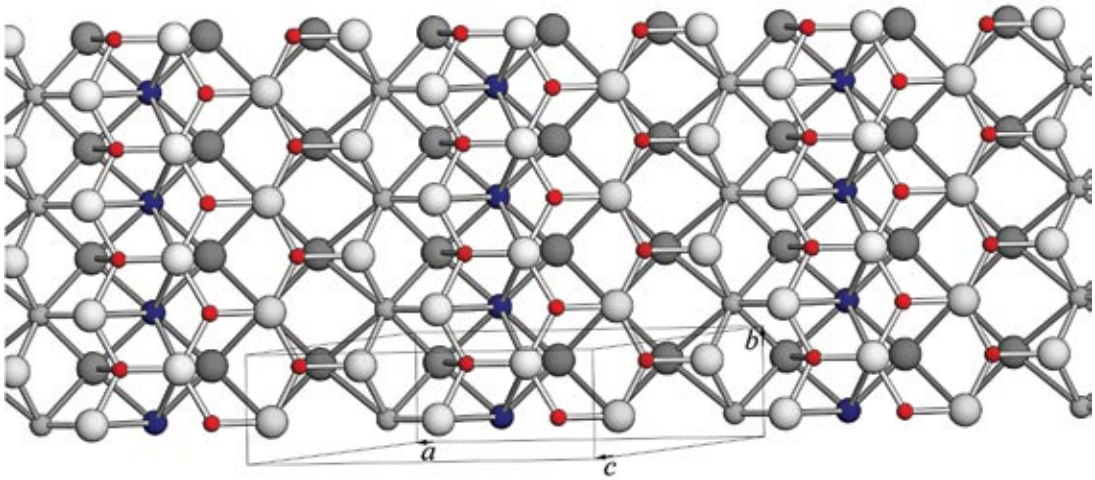

FIG. 7. Interlayer match in berryite. A pseudohexagonal layer 3^6 with subcells situated above the surface layer of the pseudotetragonal slab. Symbols as in Figure 3.

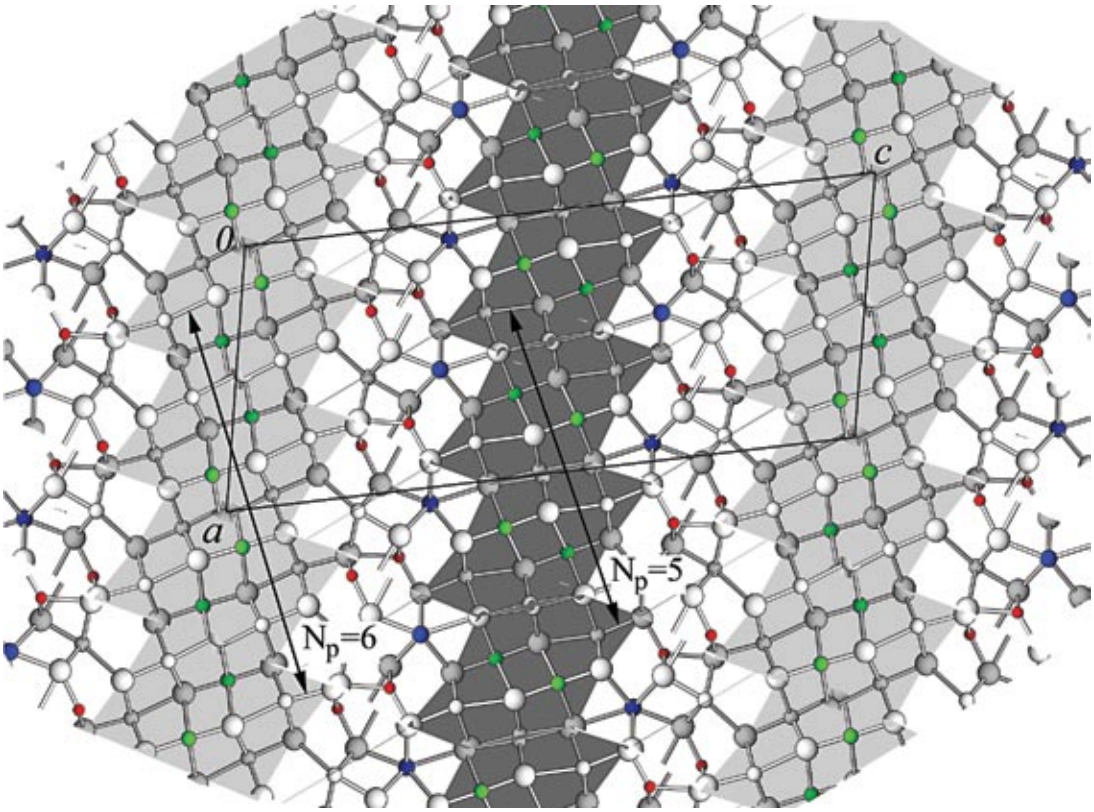

FIG. 8. Model structure of a pavonite homologue $N_P(1;2) = 5; 6$. Collage of shaded portions (a) of the berryite structure from Figure 6.

Pb–Pb decorated (in fact, lillianite-like) slabs (Fig. 8). This model concerns only the topology of the structure, whereas its chemical composition requires adjustments (*e.g.*, as $Cu_8Pb_4Ag_4Pb_2Bi_{20}S_{42}$ with Pb in two different structural roles, $Z = 1$, monoclinic, $C2/m$, with a 13.35, b 4.03, c 35.2 Å, β 105.5°).

POLYTYPISM

The berryite material from Grube Clara is monoclinic. However, the berryite material from the type specimen of cuprobismutite (U.S.N.M 92902, Missouri mine, Park County, Colorado), examined by Mumme and Makovicky, consists of a parallel intergrowth of monoclinic and orthorhombic modifications of the mineral. The pseudo-orthorhombic character of the lattice of berryite, stressed by Karup-Møller (1966), invites a closer examination of possible polytypism as well.

Marking the centerpoints of pyramidal interslab Bi–Pb pairs as vertices, "component cells" of the "Bi–Bi" and "Pb–Pb" layers can be defined (Fig. 3). The first attempt was to construct berryite variants only from one type of slab, assuming thus a possible Cu + Pb → Bi substitution. This approach does not work; as can be observed from the monoclinic structure of berryite described here, the configuration and disposition of Cu polyhedra in the pseudohexagonal layer are a function of the Bi–Pb distribution (Fig. 3). Thus, Bi–Bi or Pb–Pb pairs lead to contradictions in the Cu distribution, demanding two diametrally opposed distributions of Cu for each interval at the same time.

Therefore, viable configurations must preserve the Bi–Pb pairs in the interlayer space, and the Cu distribution as well. This leaves only one possibility, which is the presence of one kind of layer, instead of the "Bi–Bi" and "Pb–Pb" layers observed in the present structure (note that these are pairs of cations observed on pseudotetragonal surfaces). Inner portions of the "Bi–Bi" and "Pb–Pb" layers are practically identical, with the same distribution of Ag–Ag pairs and the same configuration of the Bi polyhedra. Thus, combining one half of the "Bi–Bi" layer with the opposing, matching half of the "Pb–Pb" layer is free of obvious problems.

The sequence of interlayer Bi–Pb contacts leads then to an orthorhombic structure with $a \approx 12.7$, $b \approx 4$, $c \approx 26.7$ Å, the acentric space-group $Pcm2_1$ (Fig. 9), and an unchanged chemical formula $Cu_3Ag_2Pb_3Bi_7S_{16}$, for $Z = 2$.

Analysis of Weissenberg photographs obtained from the sample of orthorhombic berryite confirms that the principal phase corresponds to the space group $Pcm2_1$, both in systematic extinctions (the *c* glide plane) and in the identity of respective F_{h0l} and F_{h2l} values (*i.e.*, disposition of atoms at $y = 0$ and ½, respectively). The distribution of *F* values in the weighted reciprocal lattice is similar to that of the monoclinic polymorph studied here. Non-overlapping reflections of the monoclinic admixture (on lattice rows with *h* odd) are slightly diffuse and spaced between the sharp reflections of the orthorhombic phase. A search for more perfect crystals of the orthorhombic polymorph, suitable for a precise determination of the structure, is under way.

The two "polymorphs" of $Cu_3Ag_2Pb_3Bi_7S_{16}$ are actually polytypes; in the polytype description, unit layers have boundaries along the central planes of the pseudotetragonal slabs; each unit layer includes (a) the pseudohexagonal S–Cu layer along its median plane, (b) the interlayer Pb–Bi configurations, and (c) two layers of atoms from each of the adjacent pseudotetragonal slabs (Fig. 3 in blue). These unit layers are polar; their polarity is given by the orientation of the Bi–Pb pairs in their median portions. In the observed structure, adjacent unit-layers are oriented in the opposite sense; in the orthorhombic model, all of them preserve the same sense. Reversal and non-reversal polytypes such as the polytypes of berryite just described do not form an OD-family (Ďurovič 1997). This situation will not be changed even if the pairs of pseudotetragonal slabs in the central layer are defined as one kind of layer and their peripheral layers plus the pseudohexagonal layers as the other kind of layer, *i.e.* as a potential polytype composed of two kinds of unit layers.

Relationship to Other Structures

Structure model for watkinsonite

Watkinsonite, $Cu_2PbBi_4(Se,S)_8$ was described by Johan *et al.* (1987) from the selenide–telluride association of the Otish Mountains uranium deposit, in Quebec. The empirical formula of the mineral is $Cu_{2.36}Pb_{1.26}$

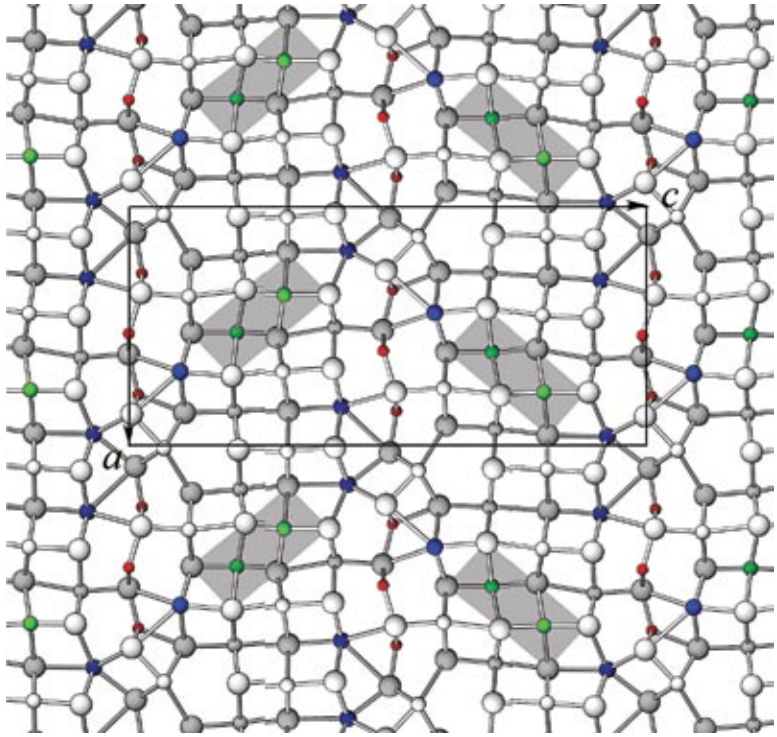

FIG. 9. A proposed structure of the orthorhombic polytype of berryite. Collage based on the structure in Figure 3. Pairs of Ag octahedra are shaded. Its derivation is described in the text.

$Bi_{3.70}(Se_{6.21}S_{1.74}Te_{0.05})$, thus suggesting a degree of the Bi + □ → Cu + Pb substitution. Johan *et al.* (1987) reported watkinsonite as being monoclinic, space group *P*2/*m*, *P*2 or *Pm*, with *a* 12.921 Å, *b* 3.997 Å, *c* 14.989 Å, β 109.2°. The crystal structure of watkinsonite was not determined at that time, and remains unknown.

Our attention was attracted by the d_{001} spacing of watkinsonite, 14.16 Å, very close to one half of the analogous spacing in berryite, 28.24 Å. It turns out that the unit cell of watkinsonite is practically identical to the "component cell" centered on the "Pb–Pb" slab in berryite (Fig. 3, the right one of the component cells outlined in red). However, the pseudohexagonal layers on two sides of the "Pb–Pb" slab in berryite are oppositely oriented, preventing a repetition by simple translation. Therefore, we assume that in watkinsonite, the layers are of the "Pb–Bi" type, and their sequence displays symmetry *Pm*.

The unit-cell content of watkinsonite according to the "Pb–Bi" berryite model is $Cu_3M_{12}S_{16}$, in contrast with $Cu_{4.8}Pb_{2.52}Bi_{7.40}S_{16}$ given by Johan *et al.* (1987). Recalculation invoking Cu-for-Bi substitution of the type observed in the pavonite series gives $Cu_3(M_{9.92}Cu_{1.80})_{\Sigma 11.72}S_{16}$, with a very good balance of charges.

The structure model for watkinsonite is different from that of orthorhombic berryite. The difference is caused by the necessity to reconstruct properly the pairs of Ag octahedra in the interior of pseudotetragonal slabs in the polytypic models of berryite; these are absent in the slabs of watkinsonite.

Related structures

To our knowledge, only two structures having modular principles analogous to berryite are known: $Ca_2Sb_2S_5$ (Cordier & Schäfer 1981) and $La_4In_5S_{13}$ (Guseinov *et al.* 1979). The monoclinic structure of $Ca_2Sb_2S_5$ (*a* 15.074 Å, *b* 5.694 Å, *c* 11.378 Å, β 110.99°, space group $P2_1/c$) shows many modular features similar to berryite (Fig. 10): PbS-like slabs four layers thick, with Sb and Ca atoms in the central layers of these slabs, and seven-coordinated Ca atoms at the surface of these slabs. The surface layers are half-occupied by cations, every second square mesh remaining unoccupied in a chessboard fashion; interlayer antimony resides above these empty squares.

The slabs are interleaved by single anionic layers of hexagonal character. In these layers, sulfur atoms

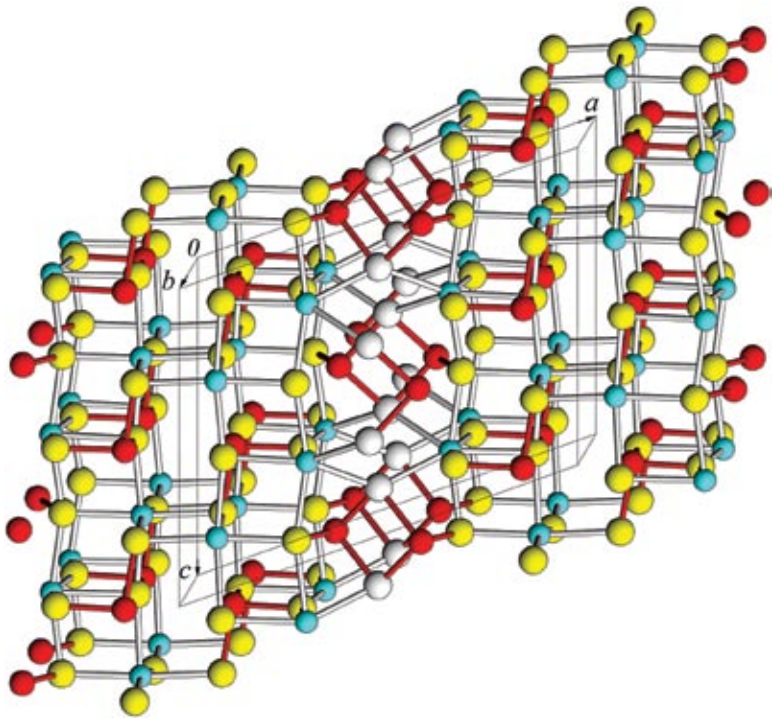

FIG. 10. The crystal structure of $Ca_2Sb_2S_5$ (Cordier & Schäfer 1981). Blue spheres: Ca, red spheres: Sb, yellow and light spheres: S.

form 6^3 nets instead of the 3^6 nets of berryite, *i.e.*, the central S atoms of hexagons are missing (Fig. 11). The interlayer Sb atoms have the two shortest bonds oriented into this layer, whereas the third shortest bond binds them to the pseudotetragonal slabs. This situation differs from berryite, in which all three short Bi–S bonds are oriented toward the hexagonal layer.

In order to achieve a simple description of the interlayer match (Fig. 11), we have to ignore the absence of some atoms of sulfur in the pseudohexagonal layer. Furthermore, we have to choose a centered pseudotetragonal mesh instead of the primitive mesh in berryite. Then, in the orthohexagonal cell description, the match is $3b_H = 2b_Q$ and $1c_H = 1c_Q$, both meshes being centered.

The crystal structure of $La_4In_5S_{13}$ (Guseinov *et al.* 1979) is orthorhombic (*a* 21.393, *b* 11.843, *c* 4.061 Å, space group *Pbam*). The combination of the coordination requirements of In^{3+} and La^{3+} leads to pseudotetragonal slabs that are three layers thick, instead of four layers in such slabs of berryite. Cations on the surface of the Q layer are the La atoms, protruding out of the square-pyramidal coordination, and tetrahedrally (or five-) coordinated In (Fig. 12).

The pseudohexagonal S layer is slightly wavy but complete, bonded both by La and four-to-five coordinated In. The interlayer match corresponds to that of berryite, *i.e.*, $2b_H = 3b_Q$ and $1c_H = 1c_Q$ (Fig. 13). Lanthanum configurations are similar to those of the paired Pb sites Pb1 – Pb3 on the surface of Q slabs of berryite, whereas the five-coordinated In site bears a resemblance to Bi1 in berryite. The most interesting point is that the lateral expansion of the Q layer, provided for in berryite by the pair of broad Ag octahedra, is assured by an In octahedron in the layer interior in $La_4In_5S_{13}$, rotated by 90° about [001] against the rest of In octahedra (Fig. 13).

"Broken-up" versions of the structural principles in berryite and $La_4In_5S_{13}$ occur in the following structures of rod-layer type: $SrBiSe_3$ (Cook & Schäfer 1982), $BaBiSe_3$ (Volk *et al.* 1980) and moëloite, $Pb_6Sb_6S_{17}$ (Orlandi *et al.* 2002). In these cases, all of which contain

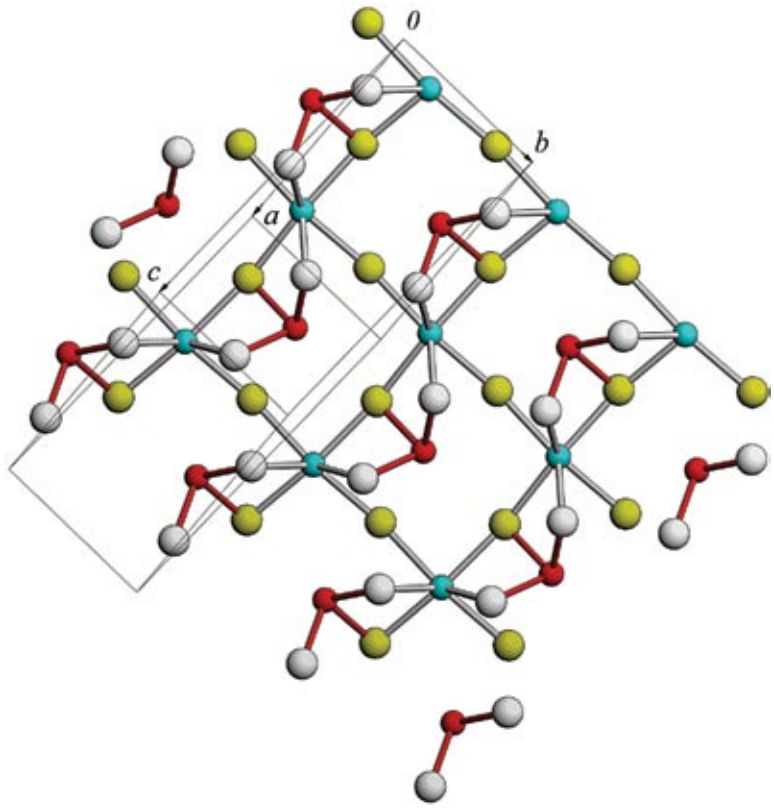

FIG. 11. Interlayer match in $Ca_2Sb_2S_5$. A pseudohexagonal layer 6^3 (S atoms: light spheres) on top of a pseudotetragonal slab (S atoms in its top layer: shaded spheres). The *a* axis points upward to the right, the *c* axis, downward to the left.

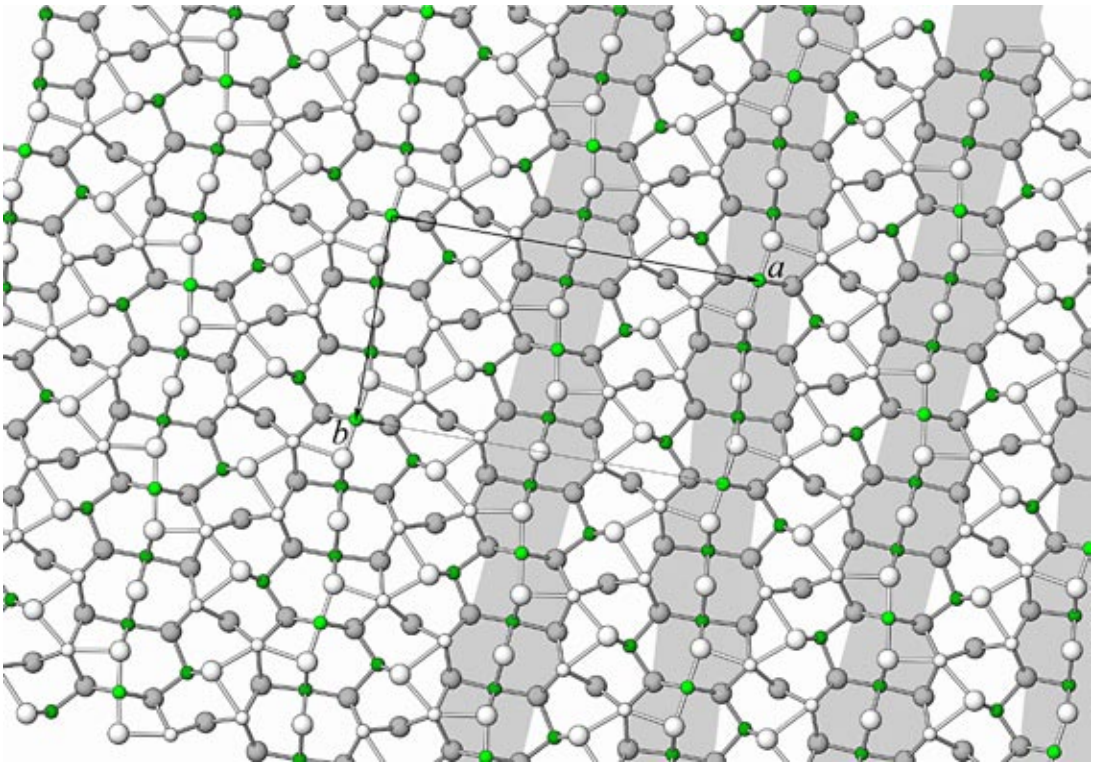

FIG. 12. The crystal structure of $La_4In_5S_{13}$ (Guseinov *et al*. 1979). Large spheres: S, green spheres: La, small spheres: In. The pseudotetragonal slabs (Q) are shaded, interleaved by a single pseudohexagonal layer (H). The *a* axis points downward, the *b* axis, toward the left.

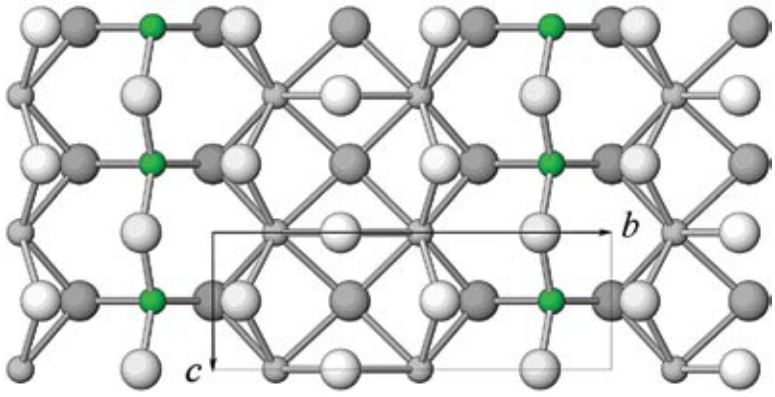

FIG. 13. Interlayer match in $La_4In_5S_{13}$. A pseudohexagonal layer 3^6 (S atoms: light spheres) on top of the surface layer of the pseudotetragonal slab (S atoms: shaded spheres). For other conventions, see Figure 12. The *b* axis is horizontal, and the *c* axis, vertical.

pseudotetragonal fragments four layers of atoms thick and fragments of single pseudohexagonal layers of anions, the charge problems are solved by covalent bonding of two or three anions (Makovicky 1993). The small problem with electroneutrality in $La_4In_5S_{13}$ might be solved by some La positions being only partly occupied.

Acknowledgements

This study was funded by the Austrian Science Foundation (FWF) through grant P 17349_N10 to the first author. This support is gratefully acknowledged. Qualified assistance of Dr. Anna Bieniok and Mrs. Camilla Sarantaris is gratefully acknowledged. Mr. A.B. Todora (Salzburg) is thanked for the stereomicroscope images. The manuscript benefitted from comments of Dr. Luca Bindi, as well as from the editorial care of Prof. Robert F. Martin.

References

Balić-Žunić, T. & Makovicky, E. (1996): Determination of the centroid or 'the best centre' of a coordination polyhedron. *Acta Crystallogr.* **B52**, 78-81.

Balić-Žunić, T. & Vicković, I. (1996): IVTON – a program for the calculation of geometrical aspects of crystal structures and some crystal chemical applications. *J. Appl. Crystallogr.* **29**, 305-306.

Borodayev, Yu.S. & Mozgova, N.N. (1971): New group of the sulfobismuthides of Ag, Pb and Cu. *Soc. Mining Geol. Japan, Spec. Issue* **2**, 35-41.

Cook, N.J. (1998): Bismuth sulfosalts from hydrothermal vein deposits of Neogene age, NW Romania. *Mitteilungen der Österreichischen Mineralogischen Gesellschaft* **143**, 19-39.

Cook, R. & Schäfer, H. (1982): Darstellung und Kristallstruktur von $SrBiSe_3$. *Revue de Chimie Minérale* **19**, 19-27.

Cordier, G. & Schäfer, H. (1981): $Ca_2Sb_2S_5$ – ein neues Erdalkalithioantimonat (III) mit Sb_2S_4 – vierringen. *Revue de Chimie Minérale* **18**, 218-223.

Ďurovič, S. (1997): Fundamentals of the OD theory. *In* Modular Aspects of Minerals (S. Merlino, ed.). *Eur. Mineral. Union, Notes in Mineralogy* **1**, 3-28.

Foord, E.E., Shawe, D.R. & Conklin, N.M. (1988): Coexisting galena, PbSss and sulfosalts: evidence for multiple episodes of mineralization in the Round Mountain and Manhattan gold districts, Nevada. *Can. Mineral.* **26**, 355-376.

Gu, Xiang-Ping, Watanabe, M., Ohkawa, M., Hoshino, K., Shibata, Y. & Chen, Desong (2001): Felbertalite and related bismuth sulfosalts from the Funiushan copper skarn deposit, Nanjing, China. *Can. Mineral.* **39**, 1641-1652.

Guseinov, G.G., Mamedov, F.H. & Mamedov, H.S. (1979): The crystal structure of $La_4In_5S_{13}$. *Dokl. Akad. Nauk Azerbaidzh. SSR* **35**, 50-53.

Harris, D.C. & Owens, D.R. (1973): Berryite, a Canadian occurrence. *Can. Mineral.* **11**, 1016-1018.

Johan, Z., Picot, P. & Ruhlmann, F. (1987): The ore mineralogy of the Otish Mountains uranium deposit, Quebec: skippenite, Bi_2Se_2Te, and watkinsonite, $Cu_2PbBi_4(Se,S)$, two new mineral species. *Can. Mineral.* **25**, 625-638.

Karup-Møller, S. (1966): Berryite from Greenland. *Can. Mineral.* **8**, 414-423.

Karup-Møller, S. (1977): Mineralogy of some Ag–(Cu)–Pb–Bi sulphide associations. *Bull. Geol. Soc. Denmark* **26**, 41-68.

Makovicky, E. (1993): Rod-based sulphosalt structures derived from the SnS and PbS archetypes. *Eur. J. Mineral.* **5**, 545-591.

Makovicky, E. (1997): Modular and crystal chemistry of sulfosalts and other complex sulfides. *In* Modular Aspects of Minerals (S. Merlino, ed.). *Eur. Mineral. Union, Notes on Mineralogy* **1**, 237-271.

Makovicky, E. & Balić-Žunić, T. (1998): New measure of distortion for coordination polyhedra. *Acta Crystallogr.* **B54**, 766-773.

Makovicky, E., Balić-Žunić, T. & Topa, D. (2001): The crystal structure of neyite, $Ag_2Cu_6Pb_{25}Bi_{26}S_{68}$. *Can. Mineral.* **39**, 1365-1376.

Makovicky, E. & Hyde, B.G. (1992): Incommensurate, two-layer structures with complex crystal chemistry: minerals and related synthetics. *Materials Science Forum* 100–101, 1-100.

Makovicky, E., Mumme, W.G. & Watts, J.A. (1977): The crystal structure of synthetic pavonite, $AgBi_3S_5$ and the definition of the pavonite homologous series. *Can. Mineral.* **15**, 339-348.

Matzat, E. (1979): Cannizzarite. *Acta Crystallogr.* **B35**, 133-136.

Nuffield, E.W. & Harris, D.C. (1966): Studies of mineral sulphosalts. XX Berryite, a new species. *Can. Mineral.* **8**, 407-413.

Orlandi, P., Meerschaut, A., Palvadeau, P. & Merlino, S. (2002): Lead–antimony sulfosalts from Tuscany (Italy). V. Definition and crystal structure of moëloite, $Pb_6Sb_6S_{14}(S_3)$, a new mineral from the Cesagiola marble quarry. *Eur. J. Mineral.* **14**, 599-606.

Sheldrick, G.M. (1997a). SHELXS97. University of Göttingen, Göttingen, Germany.

Sheldrick, G.M. (1997b). SHELXL97. University of Göttingen, Göttingen, Germany.

TOPA, D., PAAR, W.H. & ZAGLER, G. (2006): Cupromakovickyite, $Cu_8Pb_4Ag_2Bi_{18}S_{36}$, a new mineral of the pavonite homologous series. *Can. Mineral.* **44** (in press).

VOLK, K., CORDIER, G., COOK, R. & SCHÄFER, H. (1980): $BaSbTe_3$ and $BaBiSe_3$, Verbindungen mit BiSe-bzw.SbTe – Schichtverbänden. *Z. Naturforschung* **35B**, 136-140.

WALENTA, K. (1995): Neue Mineralfunde von der Grube Clara. *Lapis* **20**(5), 33-38.

Received February 7, 2005, revised manuscript accepted October 15, 2005.